Available online at www.sciencedirect.com
ScienceDirect
Mendeleev Commun., 2017, **27**, 335–337

Mendeleev Communications

Calixresorcinarene-capped silver nanoparticles as new supramolecular hybrid nanocontainers

Alina M. Ermakova,*[a,b] Julia E. Morozova,[a,b] Yana V. Shalaeva,[a,b] Victor V. Syakaev,[a] Irek R. Nizameev,[a] Marsil K. Kadirov,[a] Igor S. Antipin[a,b] and Alexander I. Konovalov[a]

[a] *A. E. Arbuzov Institute of Organic and Physical Chemistry, Kazan Scientific Center, Russian Academy of Sciences, 420088 Kazan, Russian Federation. Fax: +7 843 273 2253; e-mail: alinaermakova135@gmail.com*
[b] *Kazan Federal University, 420008 Kazan, Russian Federation*

DOI: 10.1016/j.mencom.2017.07.004

The synthesis of small (2–3 nm) silver nanoparticles in the presence of new amidoaminocarboxylic tetrapentylcalix[4]-resorcinarene and the binding of the antitumor drug Doxorubicin by a macrocycle in solution and on the surface of nanoparticles are described.

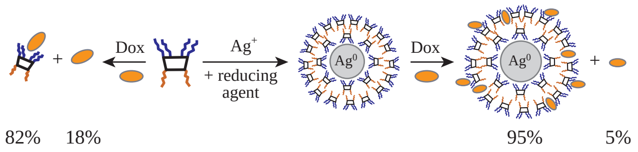

Silver nanoparticles (Ag NPs) are widely used in biology and medicine due to their antimicrobial, antifungal and antibacterial activity; recently, they were also used for targeted drug delivery.[1,2] Despite of the discussed toxicity of Ag NPs, they exhibit advantages, such as simple synthesis routes, tunable morphology,[3] high surface-to-volume ratios, intracellular delivery, and large plasmon field areas,[4,5] and can be recommended as ideal biosensors or photo-controlled delivery systems. A combination of NPs with drugs improved the efficiency, specificity, tolerability and therapeutic index of a drug.[6] The surface modification of NPs by supramolecular macrocycles significantly enhanced the characteristics of both components.[7,8] On the one hand, it increased the stability and biocompatibility of NPs and the permeability of lipid membranes to them, and, on the other hand, it improved the receptor properties of macrocycles. As a rule, amphiphilic calixresorcinarenes are low toxic; they easily stabilize the metal NPs surface through noncovalent interactions[9,10] and enhance the receptor properties owing to the cooperative effect of molecules in self-associates in solution and on the surface.[11,12] The aim of this work was to synthesize silver NPs stabilized by amphiphilic calix[4]resorcinarene, and to study the concentration of the biologically active substrate Doxorubicin (Dox) on the shells of NPs due to its binding by macrocycle molecules. Doxorubicin is a well-known anticancer drug;[13] however, its low therapeutic index requires the use of large doses that cause side effects.[1] The latter can be decreased by the concentration and targeted delivery of Dox as a part of nanocarriers (such as liposomes[13,14] and dendrimer–Dox conjugates[15,16]) or supramolecular NPs.[1]

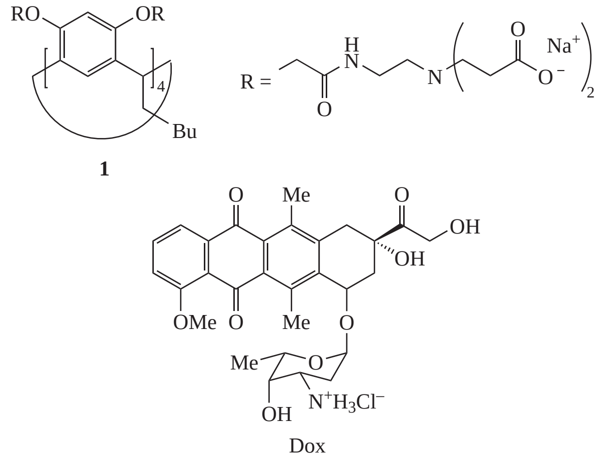

Figure 1 Structures of macrocycle **1** and Doxorubicin hydrochloride (Dox).

For the effective stabilization of silver NPs and drug binding, we synthesized tetrapentylcalixresorcinarene **1** modified with amidoaminocarboxylic groups at the upper rim (Figure 1). The carboxy groups of the macrocycle stabilize the silver NPs due to electrostatic interactions with residual silver ions on their surface, and they can participate in electrostatic interactions with the ammonium groups of Dox. The aromatic macrocycle cavity promotes π–π interaction with the anthracene moiety of Dox. Alkyl substituents in the lower rim provide hydrophobic interactions, which are necessary for the self-association of macrocycle molecules on the NPs surface *via* tail-to-tail interactions. The amino and amido groups of the upper rim substituents can form intra- and intermolecular hydrogen and donor–acceptor bonds, bringing the macrocycle closer to biological objects and providing the additional binding of Dox. The synthesis of macrocycle **1** was carried out in several steps (Figure S1, Online Supplementary Materials). Its structure was confirmed by ^{1}H and ^{13}C NMR and FTIR spectroscopy and elemental analysis (Figures S2, S3). The ^{1}H NMR spectrum of the macrocycle contains two sets of proton signals of aromatic rings (6.38, 6.81 and 5.84, 7.23 ppm, Figure S2), indicating the slow conformational boat-cone–boat exchange[17,18] in **1** due to bulky hydrophilic substituents. The boat conformation of the molecules of **1** suggests the existence of distinct hydrophilic and hydrophobic areas in the molecules that define their tendency to form self-associates in aqueous solutions. We used Fourier transform pulsed-gradient spin-echo NMR (FT-PGSE NMR) spectroscopy for determining the self-diffusion coefficients of the particles in solution. A decrease in the self-diffusion coefficient of macrocycle **1** with increasing its concentration indicates the enhancement of self-association in solution (Table 1, see Online Supplementary Materials for experimental details).

The Ag NPs stabilized by **1** were prepared by chemical reduction. An aqueous solution of sodium borohydride (0.5 mM) was added to an aqueous solution of silver nitrate (0.5 mM) and the macrocycle (0.5 mM) with stirring at room temperature.

Table 1 Self-diffusion coefficients (D_s),experimental (R_H^{exp}) and theoretical (R_H^{theor}) hydrodynamic radii and aggregation numbers (N_{ag}) of macrocycle **1** in D_2O (FT-PGSE NMR data).

C/mmol dm^{-3}	$D_s{}^a/10^{-10}$ m^2 s	R_H^{exp}/Å	R_H^{theor}/Å	$N_{ag}{}^b$
5	1.57	18	12	3
30	1.06	26		10

[a] The standard deviations of the self-diffusion coefficients did not exceed 5%.
[b] $N_{ag} = (R_H^{exp}/R_H^{theor})^3$.

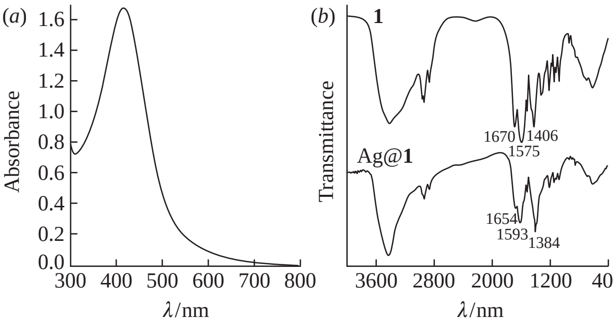

Figure 2 (*a*) Absorption spectrum of NPs Ag@**1** in water solution (in a 0.5 cm cuvette) and (*b*) IR spectra of macrocycle **1** and NPs Ag@**1**.

Immediately, the light brown color of solution appeared due to the formation of Ag NPs. The absorption spectrum of the NPs exhibited a band at 421 nm as a result of plasmon resonance in the silver NPs [Figure 2(*a*)]. In the FTIR spectra of the Ag NPs, the shifts of bands corresponding to the stretching vibrations of C–O bonds in carbonyl groups (1406 cm^{-1} for **1** and 1384 cm^{-1} for Ag@**1**) and N–H and C–N bonds in the amide groups of the macrocycle (1670, 1575 cm^{-1} for **1**, and 1654, 1593 cm^{-1} for Ag@**1**) are observed [Figure 2(*b*)]. These changes confirm the interaction of the hydrophilic groups of the macrocycle with the NPs surface. The transmission electron microscopy (TEM) images of Ag@**1** NPs reveal the occurrence of small silver NPs with a diameter of about 2–3 nm [Figure 3(*a*)]. The analysis of the Ag NPs solutions by dynamic light scattering (DLS) showed the existence of particles with an average hydrodynamic diameter of about 16 nm [Figure 3(*b*)]. The difference in the values obtained by TEM and DLS is caused by the fact that only metal clusters are reflected in the TEM images. They give a sharp contrast resulted from the high electron density of metal NPs, while the diameter of NPs in DLS is the sum of the sizes of metal particles, a macrocycle shell and a near hydrated shell. For effective stabilization, NPs should be enveloped at least by a bilayer of macrocycle molecules. In the first layer, the macrocycle molecules are oriented to the NP surface by their hydrophilic groups, and the alkyl groups of macrocycles are oriented toward the alkyl groups of the macrocycles in the second layer. The hydrophilic groups of the second macrocycle layer are located toward the aqueous layer.[9]

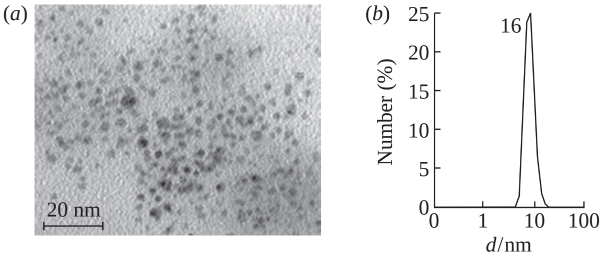

Figure 3 (*a*) TEM image of Ag@**1** and (*b*) distribution curves of NPs Ag@**1** by number, 25 °C.

Taking into account the molecular size of **1** (about 2 nm, as calculated using the ChemBio3D Ultra 11.0.1 program), the overall diameter of the NPs is about 10 nm in the case of a bilayer, which is close to the hydrodynamic diameter of the NPs obtained by DLS. Ag@**1** NPs are stable in storage for two months at room temperature (Figure S4).

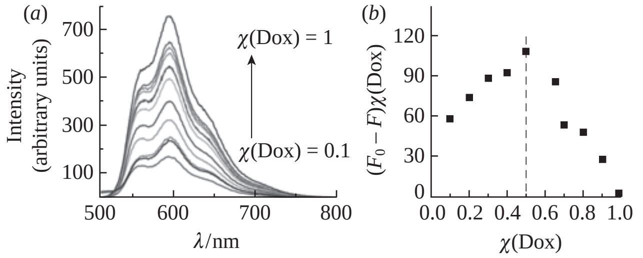

Figure 4 (*a*) Fluorescence spectra for the Job curves of **1**–Dox solutions and (*b*) Job curve for the determination of **1**–Dox complex stoichiometry.

The binding properties of macrocycle **1** and Ag@**1** toward Dox were studied by fluorimetry in a TBS buffer solution (pH 7.6). Upon light excitation at 500 nm, Dox fluoresces in a range of 520–800 nm with a maximum emission at 596 nm. In the presence of **1** or Ag@**1**, the quenching of Dox fluorescence was observed due to their interaction. The stoichiometry of complexation of **1** with Dox was determined by the continuous variation (Job) method,[19] where the total concentrations of components in solution were constant (0.05 mM), and their mole fractions varied from 0 to 1. A maximum at 0.5 in the Job curve indicates the 1 : 1 complexation in solution (Figure 4). The binding constant of Dox with **1** or Ag@**1** was found by a molar ratio method at a constant substrate concentration (0.05 mM) and varied concentrations of **1** or Ag@**1**. Figure 5 shows that the quenching of Dox fluorescence exponentially increased with the increase of concentrations of **1** or Ag@**1** in the solution.

It is well known that fluorescence quenching can occur as a result of collisions, the formation of complexes, *etc*.[20] The deviation from the rectilinear character of the $(F_0/F)/[Q]$ plot (where F_0 and F are the fluorescence of a fluorophore in the absence and in the presence of a quencher, respectively, and [Q] is the quencher concentration), and the gradient toward the *x* axis [Figure 5(*c*)] show the presence of bound and unbound fluorophores in the solution.[20] In this case, the quenching constant (association constant K) and the fraction of bound fluorophore (f_1) can be obtained from the slope and intercept of the $\{F_0/(F_0 - F)/[Q]^{-1}\}$ plot, respectively [Figure 5(*c*)]. In the Dox–**1** system, f_1 is 0.8; *i.e.*, 80% Dox is available for quenching by macrocycle **1** as a

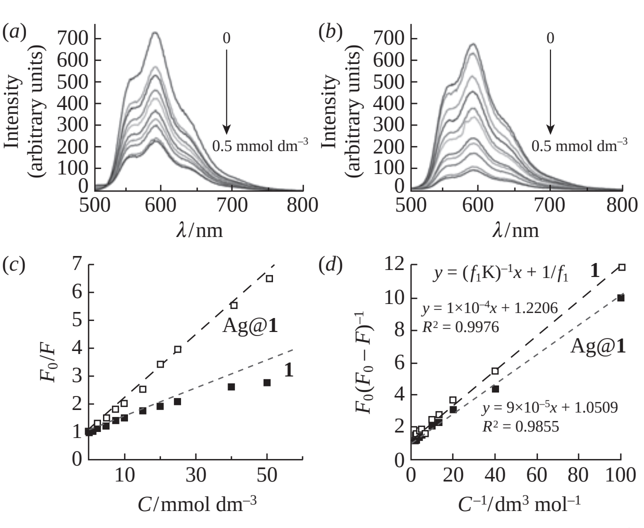

Figure 5 The wavelength dependence of Dox (C = 0.05 mmol dm^{-3}) fluorescence intensity for the solutions of (*a*) **1** and (*b*) Ag@**1** with different concentrations; (*c*) the dependence of Dox fluorescence intensity ratio in the absence (F_0) and in the presence (F) of macrocycle **1** on the concentration of the macrocycle; (*d*) $F_0(F_0 - F)^{-1}$ *vs.* C^{-1} of macrocycle for the determination of fluorophore available for quenching and quenching constant (binding).

result of host–guest complex formation; the quenching constant is 12200 dm^3 mol^{-1}. The constants of Dox association by macrocycle **1** are comparable with the binding constant (32000 dm^3 mol^{-1})[21] of Dox by mono{6-deoxy-6-thio[1-propane-3-*O*-(4-methoxyphenyl)]}-β-cyclodextrin. We suggest that it is due to possible π–π and electrostatic interactions in the Dox–**1** complex. In the presence of Ag@**1**, the quenching constant is 11700 dm^3 mol^{-1}, and the fraction of bound fluorophores is 95% [Figure 5(*d*)]. Thus, the constants of Dox association by macrocycle **1** in the solution and on the surface of silver NPs are close, but the degree of binding of guest molecules (fluorophore fraction available for quenching) increases (82 and 95%, respectively). The increasing fraction of fluorophores available for interaction with the macrocycle can be related to the ordering of the macrocycle molecules on the NPs surface; as a result, their availability for interactions with the guest molecules is increased.

Thus, the amidoaminocarboxylic derivative of tetrapentylcalix[4]resorcinarene effectively stabilizes silver NPs synthesized by chemical reduction. At an equimolar macrocycle : Ag$^+$ ratio, small (2–3 nm) Ag NPs are formed. The macrocycle binds a Doxorubicin hydrochloride substrate in aqueous solution and on the surface of NPs with close binding constants (12200 and 11700 dm^3 mol^{-1}, respectively). However, the immobilization of the macrocycle molecules on the surface of NPs enhances a cooperative effect in their self-associates, which leads to an increase of the substrate bound fraction on the surface of calixresorcinarene-capped silver NPs, as compared with the individual macrocycle solution (95 and 82%, respectively). Although additional toxicity studies are required for the hybrid nanoparticles, the combination of Ag NPs with calix[4]resorcinarene improves the stability of silver nanoparticles and the binding properties of supramolecular macrocycles.

We are grateful to Professor E. S. Nefed'ev (Kazan National Research Technological University) for performing microscopic investigations. This work was supported by the Kazan Federal University.

Online Supplementary Materials

Supplementary data associated with this article can be found in the online version at doi: 10.1016/j.mencom.2017.07.004.

References

1 F. Benyettou, R. Rezgui, F. Ravaux, T. Jaber, K. Blumer, M. Jouiad, L. Motte, J.-C. Olsen, C. Platas-Iglesias, M. Magzoub and A. Trabolsi, *J. Mater. Chem., B*, 2015, **3**, 7237.

2 C. Ganesh Kumar and Y. Poornachandra, *Colloids Surf., B*, 2015, **125**, 110.

3 A. A. Semenova, A. P. Semenov, E. A. Gudilina, G. T. Sinyukova, N. A. Brazhe, G. V. Maksimov and E. A. Goodilin, *Mendeleev Commun.*, 2016, **26**, 177.

4 A. A. Semenova, N. A. Braze, G. V. Maksimov, I. A. Semenova, A. P. Semenov and E. A. Goodilin, *Mendeleev Commun.*, 2016, **26**, 32.

5 M. O. Volodina, A. Yu. Polyakov, A. V. Sidorov, A. V. Grigorieva, E. A. Eremina, S. V. Savilov and E. A. Goodilin, *Mendeleev Commun.*, 2016, **26**, 231.

6 U. Domańska and M. Halayqa, *J. Phys. Chem. Biophys.*, 2014, **4**, 143.

7 Y. Tauran, B. Kim and A. W. Coleman, *J. Nanosci. Nanotechnol.*, 2015, **15**, 6308.

8 V. V. Spiridonov, A. N. Zakharov, I. G. Panova, A. V. Sybachin, A. A. Efimova and I. N. Topchieva, *Mendeleev Commun.*, 2015, **25**, 286.

9 M. Shen, W.-F. Chen, Y. Sun and C.-G. Yan, *J. Phys. Chem. Solids*, 2007, **68**, 2252.

10 R. Balasubramanian, B. Kim, S. L. Tripp, X. Wang, M. Lieberman and A. Wei, *Langmuir*, 2002, **18**, 3676.

11 D. A. Mironova, L. A. Muslinkina, V. V. Syakaev, J. E. Morozova, V. V. Yanilkin, A. I. Konovalov and E. Kh. Kazakova, *J. Colloid Interface Sci.*, 2013, **407**, 148.

12 Yu. E. Morozova, Ya. V. Shalaeva, N. A. Makarova, V. V. Syakaev, E. Kh. Kazakova and A. I. Konovalov, *Colloid J.*, 2009, **71**, 380 (*Kolloidn. Zh.*, 2009, **71**, 378).

13 S. A. Abraham, D. N. Waterhouse, L. D. Mayer, P. R. Cullis, T. D. Madden and M. B. Bally, *Methods Enzymol.*, 2005, **391**, 71.

14 Y. Fan and Q. Zhang, *Asian J. Pharm. Sci.*, 2013, **8**, 81.

15 Q. Zhong and S. R. P. da Rocha, *Mol. Pharmaceutics*, 2016, **13**, 1058.

16 W. She, D. Pan, K. Luo, B. He, G. Cheng, C. Zhang and Z. Gu, *J. Biomed. Nanotechnol.*, 2015, **11**, 964.

17 A. G. S. Högberg, *J. Am. Chem. Soc.*, 1980, **102**, 6046.

18 L. Abis, E. D. Dalcanale, A. Du Vosel and S. Spera, *J. Org. Chem.*, 1988, **53**, 5475.

19 K. Hirose, *J. Inclusion Phenom. Macrocycl. Chem.*, 2001, **39**, 193.

20 J. R. Lakowicz, *Principles of Fluorescence Spectroscopy*, 3rd edn., Springer, New York, 2006.

21 O. Swiech, A. Mieczkowska, K. Chmurski and R. Bilewicz, *J. Phys. Chem. B*, 2012, **116**, 1765.

Received: 1st November 2016; Com. 16/5087